NASA Orbiting Carbon Observatory: Measuring the column averaged carbon dioxide mole fraction from space

David Crisp[a], Charles E. Miller[a], Philip L. DeCola[b]
[a] Jet Propulsion Laboratory, California Institute of Technology,
4800 Oak Grove Drive, Pasadena, CA, USA 91109-8099
David.Crisp@jpl.nasa.gov, Charles.E.Miller@jpl.nasa.gov
[b] NASA Headquarters, 300 E ST SW Washington DC 20546-0001, pdecola@nasa.gov

Abstract. The NASA Orbiting Carbon Observatory (OCO) will make space-based measurements of atmospheric carbon dioxide (CO_2) with the precision, resolution, and coverage needed to characterize regional scale CO_2 sources and sinks and quantify their variability over the seasonal cycle. This mission will be launched in December 2008 and will fly in a 705 km altitude, 1:26 PM sun-synchronous orbit that provides complete coverage of the sunlit hemisphere with a 16-day ground track repeat cycle. OCO carries a single instrument designed to make co-boresighted spectroscopic measurements of reflected sunlight in near-infrared CO_2 and molecular oxygen (O_2) bands. These CO_2 and O_2 measurements will be combined to provide spatially resolved estimates of the column averaged CO_2 dry air mole fraction, X_{CO2}. The instrument collects 12 to 24 X_{CO2} soundings/second over the sunlit portion of the orbit, yielding 200 to 400 soundings per degree of latitude, or 7 to 14 million soundings every 16 days. Existing studies indicate that at least 10% of these soundings will be sufficiently cloud free to yield X_{CO2} estimates with accuracies of ~0.3 to 0.5% (1 to 2 ppm) on regional scales every month.

Keywords: Carbon dioxide, orbiting carbon observatory, NASA Earth System Science Pathfinder Program.

1 INTRODUCTION

Carbon dioxide (CO_2) is the principal man-made greenhouse gas and the primary atmospheric component of the global carbon cycle. Precise ground-based measurements of CO_2 made since the late 1950's indicate that the atmospheric CO_2 concentration has increased from ~310 to over 380 parts per million (ppm) over this period [1]. Interestingly, comparisons of these data with CO_2 emission rates from fossil fuel combustion, biomass burning, and other human activities indicate that only about half of the CO_2 that has been emitted into the atmosphere during this period has remained there. The rest has apparently been absorbed by surface "sinks" in the land biosphere or oceans [1, 2, 3]. These measurements also show that despite the steady long-term growth in the CO_2 abundance, the atmospheric CO_2 buildup varies dramatically from year to year in response to smoothly increasing emission rates. The ground-based CO_2 monitoring network does not have the spatial resolution, coverage or sampling rates needed to identify the natural sinks responsible for absorbing this CO_2 or the processes that control how their efficiency changes from year to year.

NASA's Orbiting Carbon Observatory (OCO) is an Earth System Science Pathfinder (ESSP) mission that is currently being developed to address these issues [4]. OCO will make space-based measurements of atmospheric CO_2 with the precision, resolution, and coverage needed to characterize the geographic distribution of CO_2 sources and sinks and quantify their variability over the seasonal cycle**.** The Observatory is scheduled for a December 2008 launch from Vandenberg Air Force Base in California on a Taurus 3110 launch vehicle.

During its two-year nominal mission, OCO will fly in a circular, 705 km-altitude, near-polar, sun synchronous orbit that provides global coverage of the sunlit hemisphere with a 16-day ground-track repeat cycle. The observatory carries a single instrument designed to measure the absorption of reflected sunlight by CO_2 and molecular oxygen (O_2) at near infrared wavelengths. Co-boresighted spectroscopic measurements of the CO_2 and O_2 column abundance will be analyzed to retrieve spatial variations in the column averaged CO_2 dry air mole fraction, X_{CO2}. A sensitive, stable instrument and a comprehensive ground-based validation network are being implemented to ensure that the X_{CO2} measurements have random errors and systematic biases no larger than 0.3-0.5% on regional scales. These measurements are expected to improve our understanding of the nature and processes that regulate atmospheric CO_2, enabling more reliable forecasts of CO_2 buildup and its impact on climate change. This paper provides an update on the mission design and implementation approach at roughly the half-way point in flight system development process.

2 MAKING PRECISE CO_2 MEASUREMENTS FROM SPACE

X_{CO2} can be retrieved from simultaneous, spatially-coincident spectroscopic remote sensing observations of the CO_2 and molecular oxygen (O_2) column abundances:

$$X_{CO2} = 0.20995 \times [CO_2] / [O_2] \quad (1)$$

In this expression, the column abundances, $[CO_2]$ and $[O_2]$, specify the total number of CO_2 and O_2 molecules, respectively above a given area of the Earth's surface (usually expressed in molecules/m^2). The constant, 0.20995 is the nominal, globally-averaged mixing ratio of O_2. Estimates of $[CO_2]$ and $[O_2]$ can be retrieved by analyzing the sunlight that is absorbed by these molecules as that light traverses the atmosphere before and after it is reflected by the surface. The column abundance of CO_2 can also be inferred from thermal infrared observations, but these measurements by are not ideal for monitoring surface CO_2 fluxes because they have limited sensitivity to the CO_2 abundance near the surface [4].

The OCO measurement requirements and error budgets were derived from a series of Observational System Simulation Experiments (OSSEs). These numerical experiments used CO_2 fields from existing measurements and coupled carbon-cycle chemical tracer transport models[3]. The CO_2 fields were sampled using a range of candidate orbit geometries and data acquisition strategies and then processed with a spectrum-resolving (line-by-line), multiple scattering model to generate spectrally resolved top-of-atmosphere radiances in near infrared CO_2 and O_2 bands [5, 6]. These spectra were then processed with an instrument model that simulated the spectral range, resolving power, spectral and spatial sampling, and signal-to-noise ratios of candidate instrument designs. These results were analyzed with a prototype OCO X_{CO2} retrieval algorithm to develop representative, end-to-end X_{CO2} error budget [5, 6]. This information was then used in CO_2 flux inversion models to assess the information content and CO_2 flux errors associated with the OCO measurement approach [7, 8, 9].

Precise, bias-free measurements of $[CO_2]$ and $[O_2]$ are essential for monitoring surface sources and sinks because CO_2 surface fluxes must be inferred from spatial and temporal gradients in X_{CO2}, which is thought to vary by no more than ~2% on regional to continental scales(1000 by 1000 km) [3, 7, 8, 9, 10, 11]. Our OSSEs showed that X_{CO2} measurements with precisions between 0.3 and 0.5 % (1 to 2 ppm out of the ambient ~380 ppm CO_2 mixing ratio) on regional-to-continental scales could dramatically improve our understanding of CO_2 surface fluxes. Measurements extending over at least one complete annual cycle are needed to characterize seasonal variability in CO_2.

Results from the prototype OCO retrieval algorithms confirm that estimates of X_{CO2} with the needed precision and accuracy can be retrieved from high-spectral resolution measurements of absorption by CO_2 and O_2 in reflected sunlight at near-infrared wavelengths. The weak CO_2 absorption band near 1.61 μm is well suited for CO_2 surface source/sink inversions because the absorption in this band is most sensitive to the CO_2 abundance near the

surface, where most sources and sinks are located. This spectral region is also relatively free of absorption by other gases. Co-boresighted measurements in the 0.765-μm O_2 A-band provide information about the total (dry-air) atmospheric mass, yielding clear-sky surface pressure estimates accurate to ~1 mbar over most of the sunlit hemisphere. The O_2 data will also provide constraints on the atmospheric optical path associated with pointing uncertainties, scattering by thin clouds, and aerosols, and irregular topography. Spectra of the strong CO_2 band centered near 2.06-μm band provide information about the aerosol optical properties at near-infrared wavelengths. A single *sounding* consists of three co-boresighted spectra in the 0.76-μm O_2 A-band and the CO_2 bands at 1.61 μm and 2.06 μm (Fig. 1).

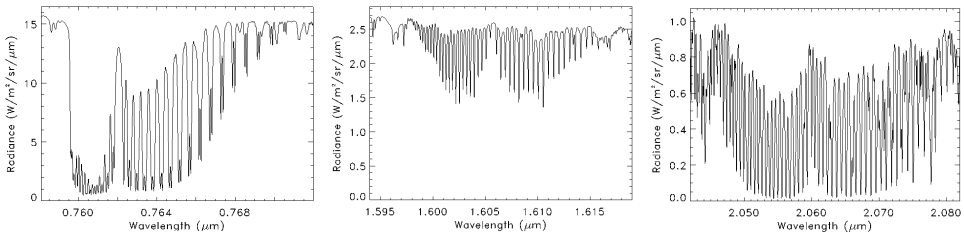

Fig. 1. The three spectral ranges sampled by the OCO instrument are shown at the nominal resolving powers.

The spectral range and resolving power for each channel were chosen to maximize the sensitivity to variations in the column abundances of CO_2 and O_2 and to minimize the impact of systematic measurement errors (Fig. 1). The OSSEs showed that a resolving power, $\lambda/\delta\lambda >$ 20,000 separates individual CO_2 lines from weak H_2O lines and from the underlying continuum in the 1.61 and 2.06-μm regions. A resolving power of ~17,000 is needed to resolve the O_2 doublets from the continuum in the 0.765-μm region. With these measurements, the retrieval algorithm can characterize the surface reflectance and solve for the wavelength dependence of the aerosol scattering throughout each spectral range, minimizing X_{CO2} retrieval errors contributed by uncertainties in these properties.

The OSSEs provided valuable insight into the spatial sampling strategy and optimal viewing geometries. Source-sink inversion experiments show that spatially-resolved measurements of X_{CO2} were needed over >90% of the sunlit hemisphere on monthly intervals to resolve the pole-to-pole gradients in X_{CO2} over the seasonal cycle [3]. The need for pole-to-pole coverage dictated a near polar orbit. Because CO_2 can vary significantly over the day [8, 9], and a single satellite in a near-polar low Earth orbit cannot cover all times of day, a sun-synchronous orbit was selected to provide results at the same time of day everywhere on Earth. An equator crossing time in the early afternoon was selected because the sun is high, maximizing the scene brightness and available signal. Early afternoon is also optimal for validating remote sensing observations of X_{CO2} against near-surface *in situ* measurements because the CO_2 is well mixed through a deep planetary boundary layer at that time of day.

Complete, spatially-contiguous coverage of the Earth's surface is not essential to characterize atmospheric X_{CO2} variations on regional scales because CO_2 is dispersed over large areas as it is mixed through the atmospheric column. However, the full atmospheric column must be sampled to provide constraints on surface CO_2 sources and sinks. Clouds and optically thick aerosols can obscure the surface, precluding measurements of the full CO_2 column. Studies of EOS MODIS cloud products and ICESAT GLAS soundings [6, 12] indicate that the probability of sampling a cloud-free scene decreases with increasing footprint size. Large topographic variations over land and other sources of spatial variation within the footprint of an individual sounding can also introduce random errors and systematic biases that compromise the accuracy of X_{CO2} retrievals. A small (<0.004 steradian) field of view was

therefore adopted to maximize the probability of viewing cloud-free scenes and to minimize the errors introduced by spatial variations within each sounding.

While the highest spatial resolution is obtained when the instrument is observing the local nadir, the OSSEs showed that this mode would yield a limited signal-to-noise ratio (SNR) over ocean or snow surfaces, which are very dark at near infrared wavelengths. A second observing mode was therefore added to view the local "glint spot", where sunlight is specularly reflected from the surface of the Earth. Glint observations provide a much higher SNR over dark surfaces. To identify and correct for biases introduced by both Nadir and Glint observations, OCO will map the entire sunlit hemisphere in Nadir and Glint mode on monthly intervals. Finally, the ability to observe stationary surface targets was added to facilitate the validation of OCO measurements against ground-based observations of CO_2. For Target observations, the spacecraft will point the instrument at a surface target as it flies overhead, acquiring observations at surface zenith angles ranging from 0° to 75°. Target observations over a range of latitudes will provide opportunities to identify and correct for biases associated with observing geometry as well as a range of geophysical parameters.

Finally, the OSSEs showed that variations in the polarization of the sunlight reflected from scenes as the Observatory moves from pole to pole along its orbit could introduce significant errors in the X_{CO2} retrievals, especially if the instrument was sensitive to polarization [14]. The Nadir and Glint observing strategies were modified to maintain a constant viewing geometry with respect to the "Principal Plane" defined by the sun, the surface footprint, and the instrument aperture, as the spacecraft proceeded along its orbit. This approach was combined with a retrieval algorithm that explicitly accounts for polarization to minimize biases introduced by polarization variations. This approach is defined further in the Section 5.

3 THE OCO INSTRUMENT

OCO carries a single instrument that incorporates three, co-boresighted, long-slit, imaging grating spectrometers optimized for the O_2 A-band at 0.765 μm and the CO_2 bands at 1.61 and 2.06 μm (Fig. 2). The instrument mass is ~150 kg, and its average power consumption is less than 165 Watts. A fast (f/1.8) optical design and a broad dynamic range were adopted to yield an acceptable SNR within small measurement footprints over the full range of viewing conditions expected over the sunlit hemisphere. The 3 spectrometers use similar optical designs and are integrated into a common structure to improve system rigidity and thermal stability. They share a common housing and a common F/1.8 Cassegrain telescope [14].

Light entering the telescope is focused at a field stop and then recollimated before entering a relay optics assembly (Fig. 2a). There, it is directed to one of the three spectrometers by a dichroic beam splitter, and then transmitted through a narrowband pre-disperser filter. The pre-disperser filter for each spectral range transmits light with wavelengths within ~±1% of the central wavelength of the CO_2 or O_2 band of interest and rejects the rest. The light is then refocused on the spectrometer slits by a reverse Newtonian telescope. Each spectrometer slit is ~3 mm long and ~25 μm wide. These long, narrow slits are aligned to produce co-boresighted fields of view that are ~0.0001 radians wide by ~0.0146 radians long. Because the diffraction gratings efficiently disperse light that is polarized in the direction parallel to the slit, a polarizer was included in front of the slit to reject the unwanted polarization before it enters the spectrometer, where it could contribute to the scattered light background.

Once the light enters a spectrometer slit, it is collimated by a 2-element refractive collimator, dispersed by a reflective planar holographic diffraction grating, and then focused by a 2-element camera lens on a 2-dimensioal focal plane array (FPA), after traversing a second, narrowband filter. The narrowband filter just above the FPA is cooled to ~180K to reject thermal emission from the instrument, which would otherwise be an important source

of noise in the 1.6 and 2.06 μm CO_2 channels. It also helps to protect against light that leaks through pinholes in the pre-disperser filter [14].

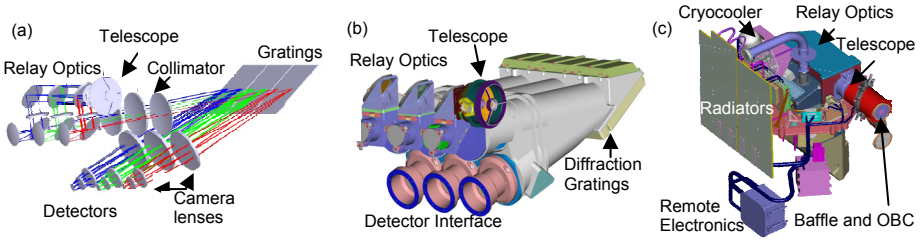

Fig. 2. Three views of the OCO instrument showing (a) the major optical components and optical path, (b) the integrated optical bench assembly, and (c) the integrated instrument with cryocooler, shrouds, radiators, and telescope baffle with on-board calibrator (OBC).

The spectral range and resolving power of each spectral channel was chosen to maximize sensitivity and minimize biases, within the constraints of the mission resources. The spectral range of each channel includes the complete molecular absorption band as well as some nearby continuum to provide constraints on the optical properties of the surface and aerosols as well as absorbing gases. To meet these requirements, the O_2 A-band channel covers 0.758 to 0.772 μm with a resolving power of ~18,000, the 1.61 μm CO_2 channel covers 1.594 to 1.619 μm, with a resolving power of ~21,000, and the 2.06 μm channel extends from 2.042 to 2.082 with a resolving power of ~21,000 [14].

The gratings disperse the light onto the FPAs in the direction orthogonal to the long dimension of the slit (Fig. 3). The field of view is resolved spatially along the slit [14]. The FPAs are 1024 x 1024 pixel arrays with 18 μm by 18 μm pixels that have 100% fill factor (i.e. there are no spatial or spectral gaps between the pixels). The full-width at half maximum (FWHM) of the slit image is sampled by 2 to 3 pixels on the FPA. The CO_2 channels use mercury cadmium telluride (HgCdTe) and O_2 A-band channel uses silicon as the photosensitive materials. Both the silicon and HgCdTe FPAs use the same read-out integrated circuit, simplifying the readout electronics. The quantum efficiency of the FPA's is between 75 and 90%, and the read noise is < 30 electrons/pixel/exposure. Thermal noise is negligible for the short exposure time (0.333 seconds). The temperatures of the CO_2 FPAs are maintained at <120 K and the O_2 FPA is maintained < 180 K by an pulse-tube cryocooler that is thermally coupled to an external radiator though variable conductance heat pipes (Fig. 2c). The body of the spectrometer maintained at ~ 5 °C by a thermal radiative shroud that is coupled to an external radiator by variable conductance heat pipes [4, 14].

The spectrum within each channel is dispersed to illuminate all 1024 pixels in spectral dimension on each FPA. The length of the slit limits spatial field of view to only ~190 pixels in the spatial dimension (Fig. 3). OCO soundings use an along-slit field of view is defined by ~160 of these 190 pixels. In normal science operations, the FPA's are continuously read out at 3 Hz. To reduce the downlink data rate and increase the SNR, 20 adjacent pixels in the FPA dimension parallel to the slit (ie. The "Spatial Direction" in Fig. 3) are summed on board to produce up to 8 spatially-averaged spectra. The along-slit angular field of view of each of these spatially-averaged "super-pixels: is ~1.8 mrad (0.1° or ~1.3 km at nadir from a 705 km orbit) [14]. The angular width of the narrow dimension of the slit is only 0.14 mrad, but the telescope focus was purposely softened to increase the effective full width at half maximum of each slit to ~0.6 mrad to simplify the boresight alignment among the 3 spectrometer slits [14].

In addition to the 8 spatially-binned, 1024-element spectra, each spectrometer also returns 4 to 20 spectral samples without on-board spatial binning to provide the full along-slit spatial

resolution. Each of these full-resolution "color stripes" covers a 220 pixel wide region of the FPA that includes the full length of the slit (190 pixels) as well as a few pixels beyond the ends of the slit (Fig. 3). These full-spatial-resolution color stripes are used to detect spatial variability within each of the spatially summed super pixels and to monitor the thermal emission and scattered light within the instrument.

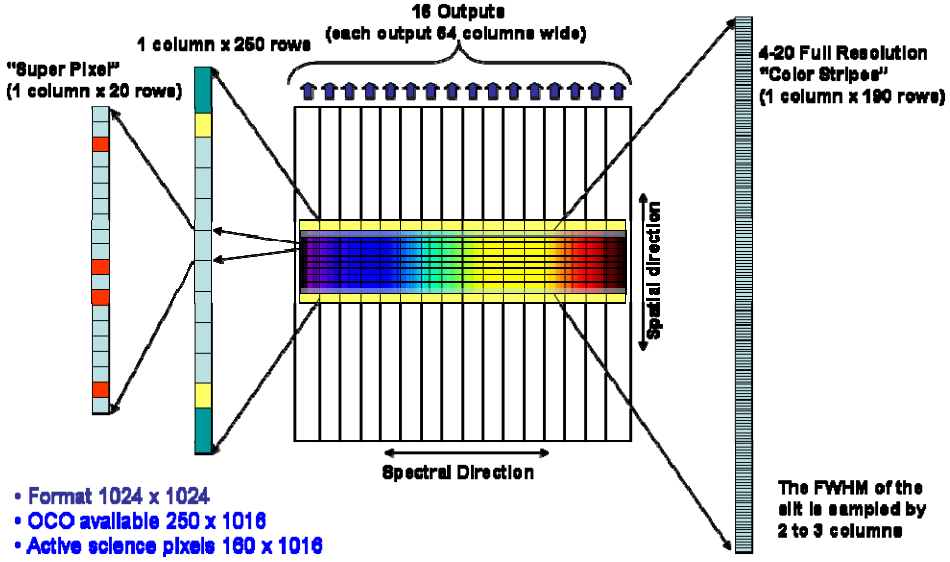

Fig. 3. The illumination and readout scheme used for the OCO Focal Plain Arrays.

An on-board calibrator (OBC) has been integrated into the telescope baffle assembly (Fig. 2c). This system consists of a calibration "propeller" that carries an aperture cover (lens cap) and a transmission diffuser. The cover is closed to protect the instrument aperture from external contaminants during launch and orbit maintenance activities. It is also closed to acquire "dark frames" that are used to monitor the zero-level offset of the FPAs. The back side of the cover has a diffusively reflecting gold surface that can be illuminated by one of 3 tungsten lamps installed in the baffle assembly. The lamp "flat field" images are used to monitor the relative gain of the individual pixels on the FPAs. The calibration propeller is rotated 180 degrees from the closed position to place the transmission diffuser in front of the aperture for direct observations of the sun. These measurements are used to perform an absolute radiometric calibration of the instrument and to acquire solar spectra for the full range of Doppler shifts (± ~7 km/sec) observed over the illuminated hemisphere. The calibration mechanism is rotated 90 degrees from either the closed or diffuser positions for normal science observations.

4 THE OCO SPACECRAFT BUS

OCO uses a dedicated spacecraft bus based on the single-string version of Orbital Sciences LEOStar-2 architecture (Fig. 4) [4, 15, 16]. This 3-axis stabilized bus supports the instrument through launch and orbit insertion, provides power, points the instrument, receives and processes commands from the ground, and records, stores, and downlinks the data collected by the instrument. The spacecraft bus consists of a hexagonal structure that is 2.12 m long and 0.94 m wide. The instrument is entirely enclosed within the upper half of the bus structure for thermal stability (Fig. 4a). The spacecraft bus has a dry mass of~315 ± 1 kg, and the observatory has a total wet mass of 460 ± 1 kg.

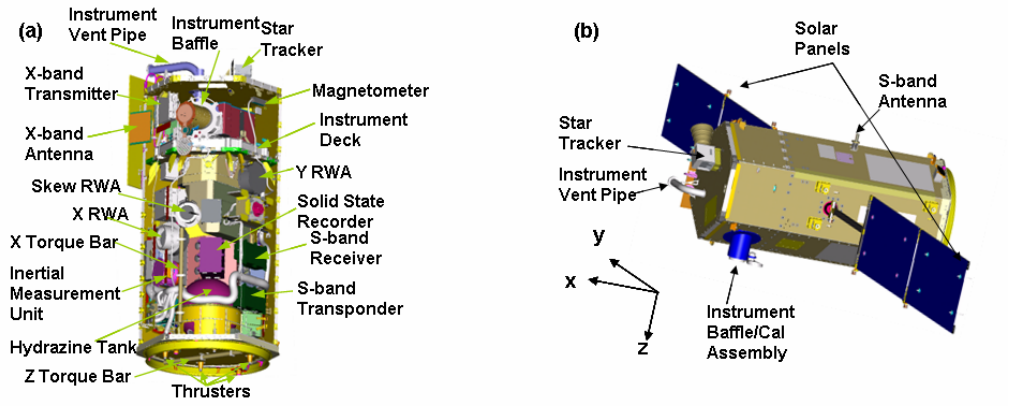

Fig. 4. (a) A cutaway view of the Observatory, showing the major components of the spacecraft bus and the location of the instrument in the upper half of the bus enclosure. The Observatory is shown in its operational configuration with its solar panels deployed. The x (roll), y (pitch) and z (yaw) axes are also shown. The solar panels rotate about the pitch axis. The long dimension (spatial direction) of spectrometer slit is aligned with the spacecraft Y-axis.

The command and data handling system manages the attitude control, power, propulsion, and telecom systems, and the 128 Gigabit solid-state recorder that stores the science data. Electrical power is provided by a pair of deployable solar panels that rotate around the pitch (y) axis of the spacecraft bus to track the sun (Fig. 4). These solar panels provide ~900 Watts (end-of-life) when illuminated at near normal incidence. They also charge a 35 Amp-hr nickel-hydrogen battery that provides power during eclipse [4, 16].

A redundant pair of S-band receivers accepts commands from the ground station through a pair of helical omni-directional antennas. An S-band transmitter returns spacecraft and instrument housekeeping data directly to a ground station or through a Tracking and Data Relay Satellite (TDRS) during critical operations (e.g. orbit injection, orbit maintenance maneuvers) and in spacecraft emergencies. During nominal operations, both science and housekeeping data are returned to the ground at 150 megabits/second using an X-band transmitter and a body-mounted X-band patch antenna.

The spacecraft bus points the instrument for science data acquisition. It also points the body-mounted X-band antenna at the ground station for data downlink. The attitude control system (ACS) uses 4 reaction wheels to control the pitch, roll, and yaw of the bus. A set of 3 magnetic torque rods is used to de-spin the reaction wheels. A star tracker, inertial measurement unit, and a magnetometer provide pointing information. A GPS receiver provides positional information along the orbit.

The bus orients the instrument to collect science observations in Nadir, Glint, and Target modes (Fig. 5) [4, 15, 16]. In Nadir mode, the satellite points the instrument aperture to the local nadir, so that data can be collected along the ground track just below the spacecraft. In Glint mode, the ACS is programmed to point the instrument aperture toward the bright "glint" spot. In Target mode, the ACS points the instrument's aperture at specific stationary surface targets as the satellite flies overhead. To ensure that the target is not missed, the ACS superimposes a small amplitude sinusoidal oscillation (±0.23° about the spacecraft y axis) in the direction perpendicular to the long dimension of the spectrometer slit, to scan the slits over a region centered on the nominal target location (Fig 5c). This "Target scan", combined with the instruments 0.8° wide field of view, creates a 0.46° by 0.8° viewing box around the target. The period of this sinusoidal oscillation will be less than 24 seconds, such that the slit is scanned over the target >20 times in a 9-minute Target observation.

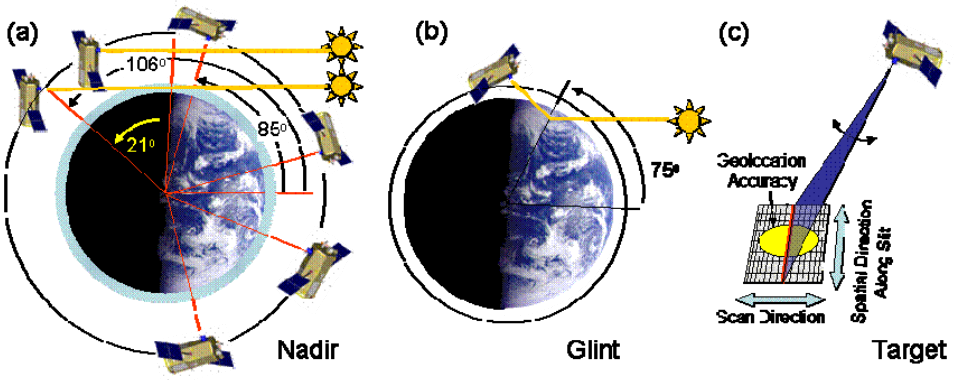

Fig. 5. Nadir, Glint, and Target observations. (a) Nadir observations are acquired over the sunlit hemisphere at latitudes where the surface solar zenith angle is less than 85°. On all orbits except downlink orbits, as the Observatory passes over the northern terminator, it pitches up to point the instrument aperture at the sun for solar radiometric calibrations. It maintains an inertial pointing until the sun sets through the Earth's limb. (b) Glint observations are made at latitudes on the sunlight hemisphere where the solar zenith angle is less than 75°. (c) For Target observations, the bus points the instrument at a stationary surface target as it flies over. A small-amplitude sinusoidal oscillation in the pitch axis is superimposed on the nominal Target pointing to scan the spectrometer slit across the Target.

For Nadir and Glint observations, the ACS is required to point the instrument's field of view to within 0.25° of its intended target (3 km at nadir). For Target observations, a pointing accuracy of 0.3° is required. Pre-launch simulations indicate that the ACS can meet these requirements with substantial margins. Ground processing of ACS data can improve the pointing knowledge to 0.1° (1250 m at nadir) for Nadir, Glint, and Target observations.

The hydrazine mono-prop propulsion system carries 45 kg of fuel to raise the orbit from the injection altitude to the operational orbit, adjust the orbit inclination as necessary, maintain the orbit during its 2-year nominal lifetime, and then de-orbit the Observatory at the end of the mission [15, 16]. Hydrazine is the only consumable resource on the Observatory. Assuming a nominal injection in to the operational orbit, there should be adequate fuel to operate the mission well beyond its nominal 2-year lifetime.

5 MISSION OPERATIONS

OCO will be launched from Vandenberg Air Force Base on a dedicated Orbital Sciences Taurus XL (3110) launch vehicle. It will initially be inserted into a 640 km altitude, near-polar, dayside-ascending (south to north) orbit. The onboard propulsion system will be used to transfer the Observatory into its operational 705 km circular orbit. This orbit transfer and other in-orbit checkout activities are expected to take less than 45 days. Once in its operational orbit, OCO will fly in the Earth Observing System (EOS) Afternoon Constellation (A-Train) [17]. The OCO orbit will be maintained with respect to Worldwide Reference System-2 (WRS-2), with a 1:26-p.m. ascending equator crossing time such that it will share its ground track with Aqua. This orbit facilitates direct comparisons and combined analyses of OCO observations with measurements taken by Aqua, Aura, CloudSat, CALIPSO, and other A-Train satellites. The orbit's 16-day ground repeat cycle facilitates monitoring X_{CO2} variations over the entire sunlit hemisphere on semi-monthly intervals. The orbit period is 98.8 minutes, yielding 14.57 orbits/day or 233 orbits every 16 days. While sequential ground tracks are

separated by ~24° of longitude, the spacing between adjacent ground tracks for the 233 orbits obtained over a 16-day ground repeat cycle is only ~1.5° of longitude.

OCO will switch from Nadir to Glint observations on alternate 16-day global ground-track repeat cycles so that the entire Earth is mapped in each mode every 32 days. Comparisons between Nadir and Glint observations will provide opportunities to identify and correct for biases introduced by the viewing geometry. Target observation will be acquired over an OCO validation site roughly once each day.

The same data sampling rate is used for Nadir, Glint, and Target observations. While the instrument is capable of collecting up to 8 adjacent, spatially resolved samples every 0.333 seconds (24 samples per second), the nominal data transmission and ground processing approach has been sized to accommodate only 12 samples per second as a cost saving measure. At this data collection rate, the Observatory collects ~200 soundings per degree of latitude as it travels from pole to pole, or ~7 million soundings over the sunlit hemisphere every 16 day ground repeat cycle. The data collection rate can be increased to 24 samples/seconds at any time during the mission if there are adequate resources. Clouds, aerosols, and other factors will reduce the number of soundings available for X_{CO2} retrievals, but existing studies suggest that at least 10% of these data will be sufficiently cloud free to yield X_{CO2} estimates with accuracies of ~0.3 to 0.5% (1 to 2 ppm) on regional scales at monthly intervals.

Nadir observations will be collected at all latitudes where the surface solar zenith angle is less than 85°. This mode provides the highest spatial resolution and is expected to return more usable soundings in regions that are partially cloudy or have significant surface topography. However, Nadir observations are expected to have limited SNR's over dark ocean- or ice-covered surfaces at high latitudes. Glint observations are expected to provide much greater SNR over these surfaces. Glint soundings will be collected at all latitudes where the surface solar zenith angle is less than 75°.

Target observations will be conducted over OCO validation sites that are within 61° of the local spacecraft nadir along the orbit track and spacecraft viewing angles between 30° west of the ground track and 5° east of the ground track. When the target is within a few degrees of the ground track, a single pass can last for up to 9 minutes, providing 6000 to 12000 soundings in the vicinity of the target. This large number of soundings reduces the impact of random errors and provides opportunities to identify spatial variability in the X_{CO2} field near the target.

While the sunlight incident at the top of the Earth's atmosphere is unpolarized, both reflection from the surface and scattering by the atmosphere can affect the polarization of the radiation field measured by the OCO instrument. These processes act primarily to reduce the intensity of the radiation that is polarized in the direction parallel to the Principal Plane. Polarization has a much smaller effect on the intensity polarized in the direction perpendicular to the Principal Plane. As noted in Section 3, the OCO instrument is only sensitive to light polarized in the direction parallel to the orientation of the long axis of the spectrometer slits. The Nadir and Glint observing strategies have therefore been designed such that the long axis of the spectrometer slits (which are roughly parallel to the Observatory y-axis) remains oriented perpendicular to Principal Plane to maximize signal and minimize polarization errors (Fig. 6a). As the Observatory ascends over the southern terminator, its x-axis is pointed north-northwest along the orbit track and the spectrometer slits are oriented almost perpendicular to the orbit track (Fig. 6b). In this orientation, the instrument collects data in a conventional push-broom fashion, where the footprint is determined by the cross-track instantaneous field of view (0.1°) and the integration time (0.333 seconds). For Nadir observations, this yields 4 to 8 cross-track footprints along the spectrometer slit with dimensions of 1.29 km by 2.25 km.

As the Observatory proceeds northward along its orbit, it rotates counterclockwise about its z axis, such that the x-axis points westward, and the long axis of the spectrometer slits are

aligned with the track just north the sub-solar latitude. At this point, each spatially-resolved surface footprint is determined by the projected width of the slit (<0.03°) and the exposure time. For Nadir observations at the sub-solar latitude, each of the footprints is ~0.4 km by 2.25 km and there is spatial overlap between footprints acquired in successive exposures by the spatial elements along the slit. The Principal Plane azimuth rotation continues as the Observatory approaches the northern terminator, where the x-axis is pointing southwest, along the orbit track, and the spectrometer slit is once again almost perpendicular to the orbit track.

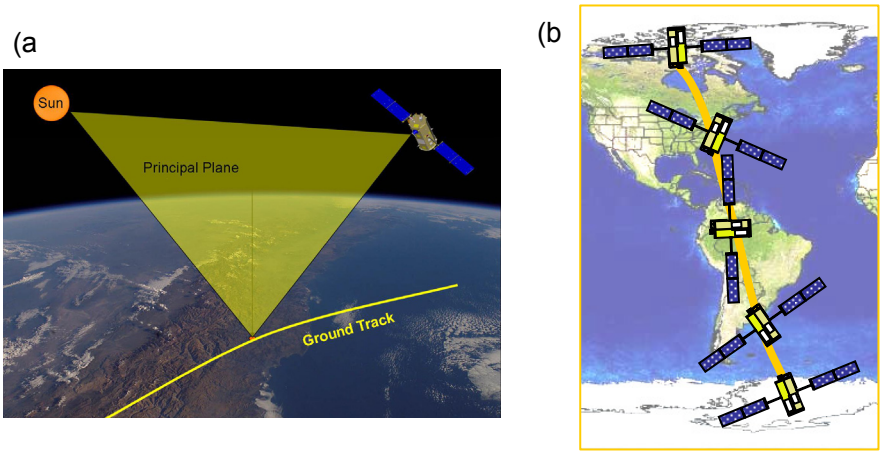

Fig. 6. (a) The Principal Plane is defined with respect to the sun, surface footprint and spacecraft. (b) The spacecraft azimuth changes during the orbit to maintain the alignment of the spectrometer slits (which are roughly parallel with the axis of the solar panels) perpendicular to the Principal Plane.

Science and housekeeping data are transmitted to a NASA Ground Network station once each day. The primary downlink station is in Poker Flats, Alaska. The backup site is in Wallops, Virginia. During a downlink orbit, the spacecraft bus points the body-mounted X-band antenna at the ground station as the spacecraft flies overhead, and data is transmitted at 150 Mbit/second for up to 9 minutes [15, 16]. A full day of science and housekeeping data can be returned in single pass, with substantial margins.

Prior to launch, the OCO instrument will be calibrated in a space simulation (thermo-vacuum) chamber to determine its radiometric, spectroscopic, and geometric response. Once in orbit, both routine and special calibration activities will be conducted to monitor changes in the instrument performance over time. Routine calibration activities to monitor the instrument radiometric and spectroscopic performance are performed on all orbits except downlink orbits. Special calibration activities are performed during the in-orbit checkout period and then every ~6 months to refine the pointing geometry and more fully characterize the instrument line shape.

Solar, Limb, Dark, and Lamp calibrations are acquired routinely. During Solar Calibration, observations of the solar disk are acquired through a diffuser to monitor the instrument's radiometric and spectroscopic performance. As the spacecraft nears the northern terminator, the on-board calibrator (OBC) is rotated 90° from its "open" position to place the transmission diffuser in front of the instrument aperture and the Observatory is reoriented to point the instrument toward the sun (Fig. 5a). The instrument will collect observations of diffuse sunlight while the sun is above the Earth's limb. These observations will be compared to pre-launch data to monitor changes in the instrument's absolute radiometric calibration. Measurements of the positions and widths of Fraunhofer lines in the solar spectrum will also be used to verify the wavelength calibration and monitor the instrument line shape (ILS) function. During Limb Calibration, the solar viewing orientation is maintained while the sun's

disk sets through the Earth's limb to provide CO_2 and O_2 spectra over a range of atmospheric paths. Spectra of narrow absorption lines in the Earth's upper atmosphere are used to further refine the wavelength calibration and to monitor the ILS in each of the 3 spectral regions.

Once in eclipse, the OBC is rotated 180° to close the aperture door for Dark and Lamp Calibration. Dark Calibration data are collected to monitor the instrument's zero level offset. The first set of Dark data is taken at the same place in every orbit, just after entering eclipse, to monitor orbit-to-orbit variations in the zero level offset of the 3 FPA's. The second set is taken at different places during eclipse to characterize zero level offset variations within an orbit. One of 3 tungsten lamps installed in the instrument's baffle assembly is used to illuminate the diffuse reflecting surface on the back side of the aperture door to produce a spatially- and spectrally uniform illumination field. The "Lamp flat fields" acquired during these Lamp Calibration activities are used to monitor and correct for instrument throughput and pixel-to-pixel gain variations on the FPAs.

The two special calibration activities are Stellar and Solar Doppler Calibrations. For Stellar Calibration, the observatory points the instrument at a bright star to verify the angular offset between the instrument boresight and the star tracker. These results are used to minimize pointing and geolocation errors. In Solar Doppler Calibration, the OBC's transmission diffuser is placed over the instrument's aperture and solar observations are collected for a full dayside orbit. These data provide solar spectral data with Fraunhofer lines that are Doppler shifted over the full range of solar radial velocities associated with the Observatory's motion in its orbit's (±7 km/second with respect to the sun). These solar spectra provide Doppler-dependent solar source for use in the X_{CO2} retrieval algorithm. They are also used to monitor variations in the ILS function in the vicinity of the solar Fraunhofer lines, which are Doppler shifted by ±2 pixels as OCO goes through its orbit.

6 THE OCO VALIDATION PROGRAM

To verify the accuracy of the space-based X_{CO2} data, the OCO project is developing a validation program that ties the space-based column CO_2 measurements with the World Meteorological Organization (WMO) standard for atmospheric CO_2. The WMO standard is based on *in situ* observations of CO_2 from flask measurements, tall towers, and aircraft. The transfer standard adopted for OCO consists of ground-based, solar-looking, Fourier Transform Spectrometers (FTS's) in the Total Carbon Column Observing Network (TCCON) [6, 11, 18, 19]. These modular, autonomous, FTS systems acquire X_{CO2} soundings using the same O_2 and CO_2 bands as the space-based OCO instrument. However, the TCCON FTS's are much less sensitive to random errors and biases than the space-based instrument. Their higher spectral resolution increases sensitivity to CO_2 and O_2 absorption and reduces biases associated with absorption by other gases within these spectral ranges. Direct observations of the solar disk reduce biases associated with aerosol scattering and other factors that contribute uncertainties in the optical path length. They also preclude uncertainties contributed by the spectral dependence of the surface reflectance and provide much higher signal to noise ratios than the space-based measurements of reflected sunlight. Most of the daily Target observations will be conducted over TCCON sites.

TCCON FTS sites are currently operating in Park Falls, Wisconsin, Lauder, New Zealand, Darwin and Wollonging Australia, Bremen Germany, and Ny-Alesund, Norway, and others are being implemented [11, 18, 19]. The OCO Project contributed the FTS systems at the Department of Energy Atmospheric Radiation Monitoring (ARM) sites near Darwin Australia and a new site to be deployed in Billings, Oklahoma. OCO is also upgrading at least 4 existing FTS facilities from the Network for Detection of Atmospheric Composition Change (NDACC) so that they can measure the CO_2 and O_2 bands sampled by the satellite. X_{CO2} results from the TCCON FTS systems at Park Falls, Wisconsin, U.S.A. and Darwin Australia were validated against *in situ* CO_2 profiles from aircraft during the summer of 2004 [18] and

in January 2006, respectively. These experiments indicate absolute accuracies of ~0.7% and precisions of <0.1%. Most of the residual error is thought to be contributed by uncertainties in the O_2 and CO_2 spectral line parameters. Precise laboratory measurements are currently being conducted to refine the strengths, widths, and positions of the absorption lines [20, 21]. These spectroscopic measurements and other refinements in the retrieval algorithms are expected to reduce the absolute errors below 0.3% before the OCO launch.

7 OCO DATA PRODUCTS

The OCO Ground Data System is located at the NASA Jet Propulsion Laboratory. There, raw radiance spectra collected by OCO (Level 0) will first be processed to yield radiometrically calibrated, geolocated spectral radiances within the O_2 and CO_2 bands (Level 1). The bore-sighted spectra for each coincident CO_2 / O_2 sounding will then be processed to estimate the column averaged CO_2 dry air mole fraction, X_{CO2} (Level 2) [15]. Other Level 2 data products to be retrieved from each sounding include the surface pressure, surface-weighted estimates of the column averaged water vapor and atmospheric temperature, and the vertical distribution and optical depth of optically-thin clouds and aerosols. These quantities will be compared to results retrieved over the ground based validation sites to yield regional-scale constraints on the space-based X_{CO2} product over the sunlit hemisphere on monthly intervals.

The OCO retrieval algorithm incorporates a forward model for generating atmospheric radiance spectra, an instrument model that simulates the instrument response, and an inverse model for refining the atmospheric state vector. The forward model is based on a spectrum-resolving (line-by-line) multiple scattering model designed to generate high resolution synthetic spectra in scattering and absorbing atmospheres [5, 6]. The instrument model simulates the wavelength-dependent radiometric performance, the spectral dispersion, ILS, scattered light, and other instrument properties that affect the measured spectra. The inverse model uses optimal estimation theory to simultaneously retrieve CO_2 and O_2 columns as well as other state properties to produce an improved fit to the observed spectra.

Six months after the start of routine science operations, Level 0 and Level 1 data products will start to be delivered to the NASA Distributed Active Archive Center (DAAC) within 6 months of acquisition by the ground station, and will be accessible to the science community [15]. Beginning 9 months after the start of routine science operations, an exploratory Level 2 data product will be delivered to the NASA DAAC. Higher level products, including gridded maps of CO_2 sources and sinks will be delivered to the DAAC as they are developed and validated.

8 SUMMARYAND CONCLUSION

The OCO spacecraft bus and instrument are currently in their final stages of integration in preparation for the upcoming space flight qualification tests and pre-flight calibration activities. If all goes as planned, the instrument will be delivered for integration with the spacecraft bus in March of 2008. The completed observatory is scheduled for delivery to the launch site in early October 2008, to support a launch in December of that year.

Acknowledgments

This work was performed by the Jet Propulsion Laboratory of the California Institute of Technology, under contract to the National Aeronautics and Space Administration.

References

[1] S. Solomon, D. Qin, M. Manning, R. B. Alley, T. Berntsen, N. L. Bindoff, Z. Chen, A. Chidthaisong, J. M. Gregory, G. C. Hegerl, M. Heimann, B. Hewitson, B. J. Hoskins,

F. Joos, J. Jouzel, V. Kattsov, U. Lohmann, T. Matsuno, M. Molina, N. Nicholls, J. Overpeck, G. Raga, V. Ramaswamy, J. Ren, M. Rusticucci, R. Somerville, T. F. Stocker, P. Whetton, R. A. Wood and D. Wratt: "Technical Summary," in: *Climate Change 2007: The Physical Science Basis. Contribution of Working Group I to the Fourth Assessment Report of the Intergovernmental Panel on Climate Change S.* Solomon, D. Qin, M. Manning, Z. Chen, M. Marquis, K. B. Averyt, M. Tignor and H. L. Miller (Eds.)]. Cambridge University Press, Cambridge, United Kingdom and New York, NY, USA (2007).

[2] J. G. Canadell, C. Le Que´re´, M. R. Raupach, C. B. Field, E. T. Buitenhuis, P. Ciais, T. J. Conway, N. P. Gillett, R. A. Houghton, and G. Marlandi, "Contributions to accelerating atmospheric CO_2 growth from economic activity, carbon intensity, and efficiency of natural sinks," *PNAS*, (2007) [doi_10.1073_pnas.0702737104]. www.pnas.org_cgi_doi_10.1073_pnas.0702737104.

[3] C. E. Miller, D. Crisp, P. L. DeCola, S. C. Olsen, J. T. Randerson, A. M. Michalak,A. Alkhaled, P. Rayner, D. J. Jacob, P. Suntharalingam, D. B. A. Jones, A. S. Denning, M. E. Nicholls, S. C. Doney, S. Pawson, H. Boesch, B. J. Connor, I. Y. Fung, D. O'Brien, R. J. Salawitch, S. P. Sander, B. Sen, P. Tans, G. C. Toon, P. O. Wennberg, S. C. Wofsy, Y. L. Yung, and R. M. Law, "Precision requirements for space-based X_{CO2} data", *J. Geophys. Res.* **112**, D10314, (2007) [doi:10.1029/2006JD007659].

[4] D. Crisp et. al., "The Orbiting Carbon Observatory (OCO) Mission," *Adv. Space. Res., 34 (4),* 700-709, (2004) [doi:10.1016/j.asr.2003.08.062].

[5] Z. Kuang, J. Margolis, G. Toon, D. Crisp, Y. Yung, "Spaceborne measurements of atmospheric CO_2 by high-resolution NIR spectrometry of reflected sunlight: An introductory study," *Geophys. Res. Lett.*, **29**, (2002) [doi:10.1029/2001GL014298].

[6] H. Boesch, G. C. Toon, B. Sen, R. Washenfelder, P. O. Wennberg, M. Buchwitz, R. de Beek, J. P. Burrows, D. Crisp, M. Christi, B. J. Connor, V. Natraj, Y. L. Yung, "Space-based Near-infrared CO_2 Retrievals: Testing the OCO Retrieval and Validation Concept Using SCIAMACHY Measurements over Park Falls, Wisconsin," *J. Geophys. Res.* **111**, D23302, (2006) [doi:10.1029/2006JD007080].

[7] P. J. Rayner and D. M. O'Brien, "The utility of remotely sensed CO_2 concentration data in surface source inversions," *Geophys. Res. Lett.,* **28***,* 175-178, (2001) [doi:10.1029/2000GL011912].

[8] D. M. O'Brien and P. J. Rayner, "Global observations of the carbon budget, 2. CO_2 column from differential absorption of reflected sunlight in the 1.61 um band of CO_2," *J. Geophys. Res.*, **107**(D18), 4354, (2002) [doi:10.1029/2001JD000617].

[9] S. C. Olsen and J. T. Randerson, "Differences between surface and column atmospheric CO_2 and implications for carbon cycle research," *J. Geophys. Res.,* **109**, D02301, (2004) [doi:10.1029/2003JD003968].

[10] D. F. Baker, A. S. Doney, and D. S. Schimel, "Variational data assimilation for atmospheric CO_2," *Tellus*, **58B**, 359–365, (2006).

[11] T. Warneke, Z. Yang, S. Olsen, J. Korner. Notholt, G. C. Toon, V. Velazco, A. Schulz, and O. Schrems, "Seasonal and latitudinal variations of column averaged volume-mixing ratios of atmospheric CO_2," *Geophys. Res. Lett.*, **32**, L03808, (2005) [doi:10.1029/2004GL021597].

[12] F.M. Breon, D. M. O'Brien, and J. D. Spinhirne, "Scattering layer statistics from spaceborne GLAS observations," *Geophys. Res. Lett.*, **32**, L22802, (2005) [doi:10.1029/2005GL023825].

[13] V. Natraj, R. J. D. Spurr, H. Boesch, Y. Jiang, and Y. L. Yung, "Evaluation of errors from neglecting polarization in the forward modeling of O_2 *A* Band measurements from space, with relevance to CO_2 column retrieval form polarization-sensitive instruments," *J. Quant. Spect. Radiat. Trans.,* **103** (2): 245-259, (2007) [doi:10.1016/j.jqsrt.2006.02.073].

[14] R. Haring, R. Pollock, B. M. Sutin, and D. Crisp, "The Orbiting Carbon Observatory instrument optical design," *Proc. SPIE*, **5523**, 51-62, Current Developments in Lens Design and Optical Engineering V; Pantazis Z. Mouroulis, Warren J. Smith, R. Barry Johnson; Eds. (2004).
[15] D. Crisp, "OCO: Orbiting Carbon Observatory," *Earth Science Reference Handbook, a Guide to NASA's Earth Science Program and Earth Observing Satellite Missions*, C. L. Patterson, A. Ward, and M. D. King, Eds. 197-201, (2006).
[16] OCO Web Site: http://oco.jpl.nasa.gov.
[17] M. R. Schoeberl, "The Afternoon Constellation: A formation of Earth observing systems for the atmosphere and hydrosphere," *Geoscience and Remote Sensing Symposium IEEE International*, **1**, 354-356, (2002) [doi:10.1109/IGARSS.2002.1025038].
[18] R. A. Washenfelder, G. C. Toon, J.-F. Blavier, Z. Yang, N. T. Allen, P. O. Wennberg, S. A. Vay, D. M. Matross, B. C. Daube, "Carbon dioxide column abundances at the Wisconsin Tall Tower site," *J. Geophys. Res.*, **111** (D22): Art. No. D22305 (2006) [doi: 10.1029/2006JD007154].
[19] The Total Carbon Column Observing Network. "http://tccon.caltech.edu".
[20] R. A. Toth, L.R. Brown, C.E. Miller, V.M. Devi, D.C. Benner, "Line strengths of $^{12}C^{16}O_2$: 4550–7000 cm^{-1}," *J. Mol. Spect.* **239** (2): 221-242, (2006) [doi:10.1016/j.jms.2007.03.005].
[21] : R. A. Toth, L.R. Brown, C.E. Miller, V.M. Devi, D.C. Benner, "Self-broadened widths and shifts of $^{12}C^{16}O_2$: 4750–7000 cm^{-1}," *J. Mol. Spect.* **239** (2): 243-271, 2006 [doi:10.1016/j.jms.2006.08.001].

David Crisp is a Senior Research Scientist at the Jet Propulsion Laboratory/California Institute of Technology and the Principle Investigator of the NASA Orbiting Carbon Observatory mission. Since receiving his Ph.D. in Geophysical Fluid Dynamics from Princeton University in 1984, he has developed radiative transfer algorithms for remote sensing and climate models of Venus, Earth, and Mars. He has served on the science teams of several NASA missions and as the Chief Scientist of the NASA New Millennium Program from 1997 to 2001.

Charles E. Miller is a Project Scientist at the Jet Propulsion Laboratory/California Institute of Technology and the Deputy Principle Investigator of the NASA Orbiting Carbon Observatory mission. Since receiving his Ph.D. in Physical Chemistry from UC Berkeley in 1991, he has focused primarily on atmospheric chemistry and molecular spectroscopy.

Philip L. DeCola is the Program Scientist for the Aura Mission, the Atmospheric Composition Focus Area, and the Earth System Science Pathfinder (ESSP) Program in the Science Mission Directorate at NASA Headquarters. He also serves as the co-Chair of the U.S. Government's Climate Change Science Program Sub-group on Atmospheric Composition. Since receiving his Ph.D. in Chemical Physics from the University of Pennsylvania in 1990, his research has focused on molecular spectroscopy, condensed phase energy transfer, nonlinear spectroscopy and radiative transfer in planetary atmospheres.